

Electronic Supporting Information

Site-Specific Growth of Polymer on Silica Rods

Bo Peng,^{*a} Giuseppe Soligno,^b Marlous Kamp,^a Bart de Nijs,^a Joost de Graaf,^a Marjolein Dijkstra,^a René van Roij,^b Alfons van Blaaderen,^{*a} and Arnout Imhof^{*a}

^a Soft Condensed Matter, Debye Institute for Nanomaterials Science, Utrecht University, Princetonplein 5, 3584 CC Utrecht, The Netherlands

* E-mail: pengbo006@gmail.com; A.vanBlaaderen@uu.nl; A.Imhof@uu.nl

^b Institute for Theoretical Physics, Center for Extreme Matter and Emergent Phenomena, Utrecht University, Leuvenlaan 4, 3584 CE Utrecht, The Netherlands

Table of Contents

Experimental section	3
Materials	3
Procedure for silica rods synthesis.....	4
Procedure for TPM coating.....	5
Procedure for hybrid polymer-silica particles synthesis.....	5
Purification of the hybrid particles from the polar solvent	7
Procedure for dying the particles	7
Characterization	8
Electric field.....	9
Experimental results	11
Vectorial orientation of lollipop particles	20
Numerical evaluation of rod-liquid adsorption surface free energies	21
Rods with homogeneous surface properties	21
Rods with heterogeneous surface properties	27
Supplementary references	31

Experimental section

Materials

In the synthesis of silica rods: tetraethyl orthosilicate (TEOS, 98%, Aldrich) was used as the precursor for the silica rods. Ammonia (NH₃, 29 wt% solution in water, Merck) was used as the catalyst. Poly(vinylpyrrolidone) (PVP, K-30, Aldrich) with an average molecular weight of 40,000 g/mol, 1-pentanol ($\geq 99\%$, Sigma), ethanol (chemical grade, Baker), and sodium citrate dihydrate ($\geq 99\%$, Sigma) were used as received. De-ionized water was used in all experiments and was obtained from a Millipore Direct-Q UV3 reverse osmosis filter apparatus.

In the preparation of hybrid particles: Methyl methacrylate (MMA, Aldrich) was passed over an inhibitor removal column (Aldrich) at room temperature. After the inhibitor was removed, MMA was stored in a refrigerator at +4 °C for not longer than 1 month. Styrene (St, Fluka) was passed through a homemade activated alumina filled column to remove the inhibitor and used immediately. Azo-bis-isobutyronitrile (AIBN, Janssen Chimica) was re-crystallized from ethanol before use. Poly(vinylpyrrolidone) (PVP, K-90, Fluka) with a molecular weight of 360,000 g/mol and PHSA-g-PMMA (a poly(12-hydroxystearic acid) (PHSA) grafted PMMA copolymer) were used as stabilizers. The PHSA-g-PMMA stabilizer, dissolved in a mixture of ethyl acetate and butyl acetate, was homemade and its synthesis is described by Antl *et al.*^{s1} Rhodamine b isothiocyanate (Aldrich) was used as fluorescent dye. 1-Octanethiol ($\geq 98.5\%$, Aldrich), methanol (chemical grade, Biosolve), acetone (chemical grade, Baker), hexane (chemical grade, Biosolve), dodecane ($> 99\%$, Sigma-Aldrich), sulfuric acid (95%, Fisher), and hydrogen peroxide (35% in water, Merck) were used as received.

3-(Trimethoxysilyl) propyl methacrylate (TPM, 98%, Aldrich) was used as the coupling agent between silica rods and PMMA. Hydrofluoric acid (HF, 48 wt% in H₂O, Sigma-

Aldrich) was diluted to about 5 wt% with de-ionized water and then used to selectively etch the silica rods.

Procedure for silica rods synthesis

The silica rods were synthesized using the method detailed in previous papers.^{30, 33} Typically, bullet-shaped rods with a length of 737 nm and a diameter of 384 nm were prepared as follows: 80 ml of PVP (K-30) was dissolved in 800 ml of 1-pentanol by sonication until all PVP was dissolved, and placed in a 1 L glass flask. Then, 80 ml of ethanol, 40 ml of de-ionized water and 8 ml of 0.18 M sodium citrate dihydrate aqueous solution were added to the PVP/pentanol mixture. The flask was shaken by hand for 2 min. Subsequently, 16 ml of ammonia was added, and the flask was shaken again by hand. Then, 8 ml of TEOS was added to the mixture, and briefly shaken to mix the content. The flask was left to rest and the reaction was allowed to proceed for 36 h. The length of the rods can be readily tuned by using various amounts of water. More details can be found in refs. 30 and 33. After the reaction the silica rods were thoroughly cleaned by centrifugation and re-dispersion in ethanol by sonication 4 times, and finally dried with a nitrogen stream at room temperature.

The morphology of the rods can be easily tuned by growing silica layers in a precise way using seeded growth.^{30, 33, 37} For the 15 nm thick silica layer, 0.4 g of silica rods was dispersed by sonication in a mixture consisting of 40 ml ethanol, 1.3 ml water and 1.6 ml of ammonia. Then, 0.2 ml of TEOS was added. The reaction was allowed to proceed for 24 h. For the rods with two rounded ends, a ~150 nm thick silica layer was grown on the original silica rods. This process can be achieved through a multi-step growth of silica layers using in total of 7 ml TEOS. The final products were washed three times with ethanol and dried at room temperature.

In one experiment the rods were treated with a piranha solution (sulfuric acid and hydrogen peroxide at a 3:1 v/v ratio) to clean their surface from organic residues. First, the

dried rods (~ 0.05 g) were dispersed in sulfuric acid (~ 9 ml) by sonication. Then, hydrogen peroxide (~ 3 ml) was added to the suspension of rods, and the dispersion was stirred overnight. The next day, the rods were separated by centrifugation and rinsed with de-ionized water until the pH was close to 7. Finally, the rods were dried at room temperature for further use.

Procedure for TPM coating

To provide a basis for the PMMA to react to, the silica rods were treated with the coupling agent 3-(trimethoxysilyl) propyl methacrylate (TPM). Typically, 0.3 g of dried rod-like silica particles were dispersed in 5 ml of ethanol after which 1 ml of ammonia and 3 ml of TPM were added. The mixture was sonicated for 1 min to disperse the rods. The mixture was then stirred for 3 h at a moderate stirring rate (~100 rpm) at room temperature. After this procedure, the suspension was transferred to a 50 ml round bottom flask and vacuum distilled at room temperature to promote the condensation reaction as Philipse *et al.*^{s2} described. After about 20 min, 1-2 ml bright, gel-like suspension remained at the bottom of the flask, and the distillation was stopped. This TPM grafted silica (named TPM-SiO₂) was purified by 3 cycles of centrifugation/re-dispersion in methanol. The final samples were dispersed in methanol and stored at +4 °C for no longer than one week.

Procedure for hybrid polymer-silica particles synthesis

Hybrid PMMA-silica particles were synthesized through the co-polymerization of TPM grafted silica rods with methyl methacrylate (MMA) in a polar medium. Typically, a mixture containing 0.4 g PVP (K-90), 0.051 g TPM-SiO₂ rods, and 4.1 g methanol was prepared. Then, MMA containing 1 wt% of initiator (AIBN) was added. This reaction mixture was deoxygenated for 1 h by bubbling nitrogen through the mixture. Subsequently, the flask with this mixture was placed in a pre-heated silicone oil bath and maintained at 55 °C, and stirred at 100 rpm for 24 h before cooling down to room temperature. The obtained particles were

rinsed three times with methanol using a centrifuge (Hettich Rotina 46 S, at 315 g for 20 min). The products were stored in methanol for further purification to remove the free polymer particles by sedimentation. By simply scaling up the reaction (*e.g.*, five times the initial quantities), the yield of the rods increased, while the quality remained the same, and the result is shown in Figure S1a.

Hybrid PS-silica particles were synthesized in a similar way to that of PMMA-silica particles. In detail, 0.1 g PVP (K-90), 0.05 g TPM-SiO₂, and 4.1 g ethanol mixed homogeneously by sonication for 1 min, and then, St (~ 0.24 g) containing 1.2 wt% of initiator (AIBN) was added to the mixture. A de-oxygenation (N₂ bubbling through the mixture for around 1 h) was carried out prior to the co-polymerization. Co-polymerization took place at 70 °C, and was continued for 24 h. The products were washed with ethanol at 315 g for 20 min (Hettich Rotina 46 S) three times to remove the un-bonded stabilizer and monomer, and stored in ethanol for further purification to remove the free polymer particles. The result is shown in Figure S1b.

Based on the recipe aforementioned recipe, a variety of hybrid particles was successfully prepared by making use of silica rods that had undergone diverse treatments. To selectively remove the silica from hybrid particles, hydrofluoric acid (HF) was used and diluted to about 5 wt% with de-ionized water first. Then, HF aqueous solution was added in excess to the suspension of hybrid particles (~ 0.1 wt% in water), and kept stirring (~ 100 rpm) for 30 min. Subsequently, the particles were rinsed three times with de-ionized water to purify the residue of the hybrid particles, and the final product was stored at room temperature for characterization.

In the dispersion polymerization where silica rods rather than PVP acted as the stabilizer, the procedure was similar to the dispersion polymerization just described. Typically, 0.05 g of TPM-SiO₂ rods was dispersed in 4.1 g of methanol. Then, various

amounts of MMA containing 1wt% (based on the monomer mass) of AIBN were fed into the dispersion of rods under constant stirring (~ 100 rpm). After 1 h of deoxygenation, the flask was immersed in the silicone oil bath at 55 °C and maintained for 24 h. After the reaction was complete, the un-reacted MMA was removed by three rinse cycles with methanol, and the obtained product was stored in methanol for observation.

Purification of the hybrid particles from the polar solvent

The synthesis of hybrid particles also results in a number of free PMMA particles. In order to purify the hybrid particles, a mixture of glycerin and water was used in combination with a centrifuge (Hettich Rotina 46 S), to separate the hybrid particles from the mixed system. An empirical weight ratio (α) between glycerin and water was used, calculated by:

$$\alpha = \frac{\rho_g \rho_w - \rho_m \rho_g}{\rho_m \rho_w - \rho_g \rho_w} \quad (\text{S1})$$

where ρ_g , ρ_w and ρ_m are the density of glycerin (1.261 g/cm³), water (0.997 g/cm³) and mixture of glycerin and water at 25 °C, respectively. Considering the density of PMMA of about 1.18 g/cm³, we selected the density of the mixture ($\rho_m = 1.20$ g/cm³) to be slightly higher than PMMA. The separation was carried out with a Hettich Rotina 46 S centrifuge, at 800 g for 5 hours. After the third purification, the particles dispersed in methanol and centrifuged three times to remove the remainder of the glycerin/water mixture. Ultimately, the obtained particles were stored in methanol for future use.

Procedure for dying the particles

The as-synthesized hybrid particles were labeled with a fluorescent dye. First, an amount of hybrid particles (~ 0.1 g) was collected through a centrifugation process and the supernatant was removed. Then, the hybrid particles were dispersed by sonication in 5 ml of pentanol containing 1 mM of Rhodamine b isothiocyanate (RITC) in a 20 ml glass vial. The suspension was stirred at 100 rpm for 2 days at room temperature. Subsequently, the labeled particles

were washed twice with pentanol, once with methanol, and three times with de-ionized water, respectively, by centrifugation. After drying under a nitrogen stream at room temperature, the fluorescently labeled hybrid particles were stored in a dark glass vial for further observation.

In order to minimize interference from light scattering, refractive index matching between the particles and solvent is desired. However, due to the fact that the particles are made of two types of materials, fully refractive index matching is impossible. Considering the refractive index of silica (1.45) and PMMA (1.49), we chose a mixture of glycerin and water (roughly 9:1 in weight)^{s3} to refractive index match with the silica rods.

In fact, the following confocal scanning laser microscopy observation indicated that the dye only partly penetrated into the particles, developing core-shell fluorescently labeled particles (see the inset in Figure 1d).

Characterization

To determine the details (size, polydispersity and morphology and internal structure) of the particles, transmission electron microscopy (TEM) was performed with a Philips Tecnai 10 (accelerating voltage ≤ 100 kV). A diluted sample suspension was deposited on a copper grid coated with a polymer membrane which was carbon coated, and the sample was allowed to dry at room temperature. Tomographic reconstructions were made by taking TEM images at angles ranging from -70° to $+70^\circ$ with intervals of two degrees and aligned using gold markers. The software used for alignment and reconstruction is the IMOD package made by the Boulder laboratory in Colorado.^{34, 35} For the Tomogram generation the SIRT algorithm was used with 70 iteration steps and a radial filter cut-off of 0.4 and falloff of 0.05.

Scanning electron microscopy (SEM) was carried out with a Philips XL30FEG microscope to observe the surface morphology and shape of the particles. The samples were prepared by placing a drop of dispersion on a grid and allowing the solvent to evaporate at

room temperature. The samples then were sputter-coated with a layer of platinum (Pt) about 3 nm.

Confocal scanning laser microscopy (CSLM) was used to help assess the structure of the fluorescently labeled hybrid particles. The dried fluorescently labeled particles (~ 0.01 g) were dispersed in the mixture of glycerin of water (~ 1 g, 9:1 in weight) in a small vial (contents ~ 1 ml) with the help of a sonication bath. To be able to use the cell in the CSLM setup, the bottom of the vial was removed and replaced with a thin cover glass, which was glued to the vial using epoxy glue. A Nikon confocal scanning laser can head (Nikon C1) was operated in fluorescence mode on a Leica (DM IRB) inverted microscope. Measurements were performed with a Leica 100 \times oil confocal immersion lens with a numerical aperture of 1.4. The fluorescent particles were excited at around 543 nm, and their images were observed at emission wavelengths of around 605 nm.

Electric field

Electric cells were prepared from capillaries with inner dimensions 0.1 \times 1 \times 5 mm. These capillaries had been treated with 3-trimethoxypropylsilylmethacrylate prior to use, to counter the sticking of particles to the capillary walls. Wire electrodes from Goodfellow (diameter 0.05 mm and composition 95% Ni, 5% Al/Mn/Si) were spanned along the sides. A HP 33220A 15 MHz Function/Arbitrary Waveform Generator provided sinusoidal electric fields with 2V peak-to-peak voltage. A Krohn-Hite 7602M Wideband Amplifier was used for amplification of the signal to 15-20V.

The electric cells were filled with a dispersion of lollipop particles in ethanol. This dispersion was prepared from an aqueous dispersion by centrifugation, exchange of solvent, and sonication in a Branson 2510 sonication bath. The dispersion was used directly after preparation, since ethanol etches away the PMMA sphere in the course of a day. Prolonged storage in water also seemed to reduce the described vectorial orientation in the electric field.

Electric field experiments were recorded on a Leica SP8 confocal microscope. This microscope was equipped with a Plan Apo 63x oil immersion lens ($NA = 1.32$). Wavelengths of 495 nm and 543 nm were selected from the spectrum of a white light laser by means of an acousto-optical beam splitter (AOBS). Two detectors recorded in different imaging modes: a PMT in reflection mode, and a more sensitive hybrid detector in fluorescence mode. The fluorescence channel captured photons from a wavelength range about the emission maximum of the rhodamine dye. The reflection channel was set to capture light of wavelength 495 nm. In other words, this channel recorded scattering of light of 495 nm by the particles. Scattering occurs due to the refractive index match mismatch between the solvent ($n = 1.362$) and the particles (silica rods: $n \sim 1.45$, PMMA spheres: $n = 1.49$). We were able to tune the gain of both channels such that only the spheres were visible in reflection mode, due to the larger refractive index mismatch between the PMMA spheres and solvent as compared to the silica rods and solvent. The silica rods were visible in the fluorescence channel. The two channels were displayed in different 8-bit color look-up tables: reflection mode in green and fluorescence mode in red. The final images were acquired by overlaying these two channels.

We worked with AC fields rather than DC fields to eliminate (1) gathering of the particles at the electrodes and (2) solvent hydrolysis. Frequencies of about 0.5 Hz appeared slow enough to allow vectorial orientation. We needed at least five images per second for accurate sampling of the motion. For this reason, scanning was bidirectional and at a speed of 1400 Hz, while the images had a rectangular shape with a resolution of 1024 by 512 pixels. With these settings, the scanning rate was 5.24 frames/s.

Experimental results

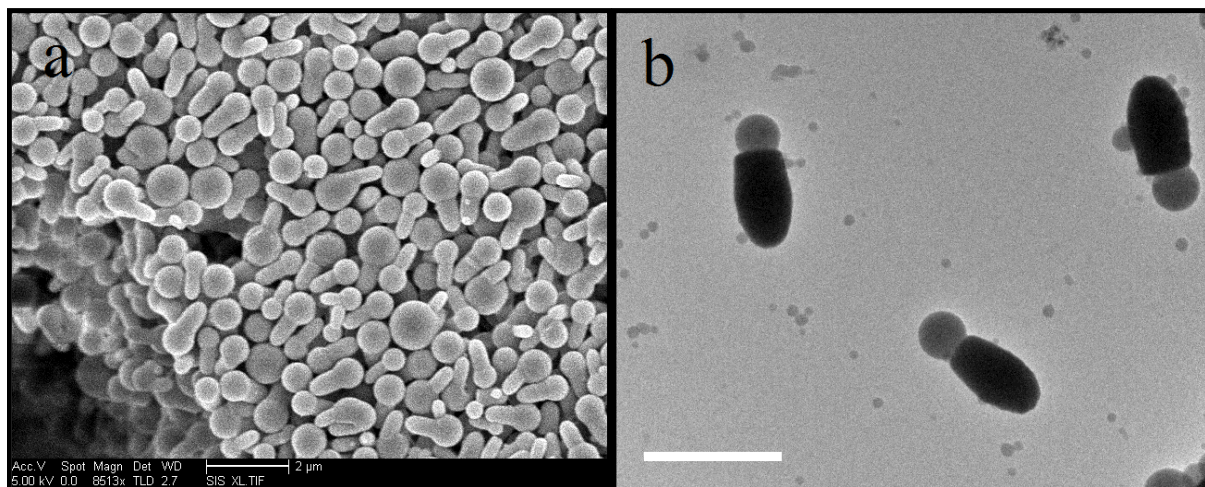


Figure S1. a, Scanning electron microscopy (SEM) image of non-spherical hybrid silica-PMMA particles prepared in bulk by using the monomer (methyl methacrylate, MMA) and rods at a weight ratio of 4.85:1. This result was obtained by scaling up by five times the recipe mentioned in the experimental section. **b**, Transmission electron microscopy (TEM) image of lollipop-shaped hybrid particles prepared by using styrene and rods at a weight ratio of 4.85:1. The scale bars are 2 μm.

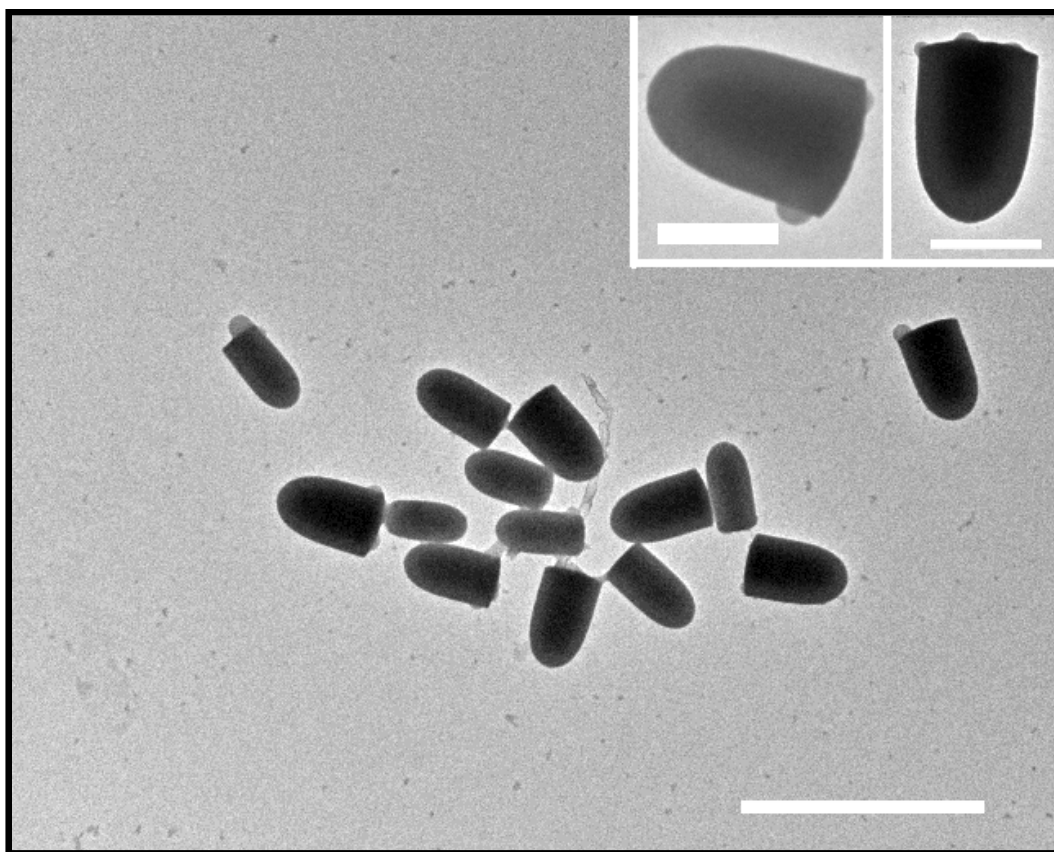


Figure S2. TEM image of hybrid particles obtained 20 minutes after the start of the polymerization of MMA in the presence of silica rods as seeds. It clearly indicates that primary nuclei of monomer were preferentially, but not exclusively, attached to the flat ends of the silica rods. The scale bars are 2 μm in the main figure and 500 nm in the insets, respectively.

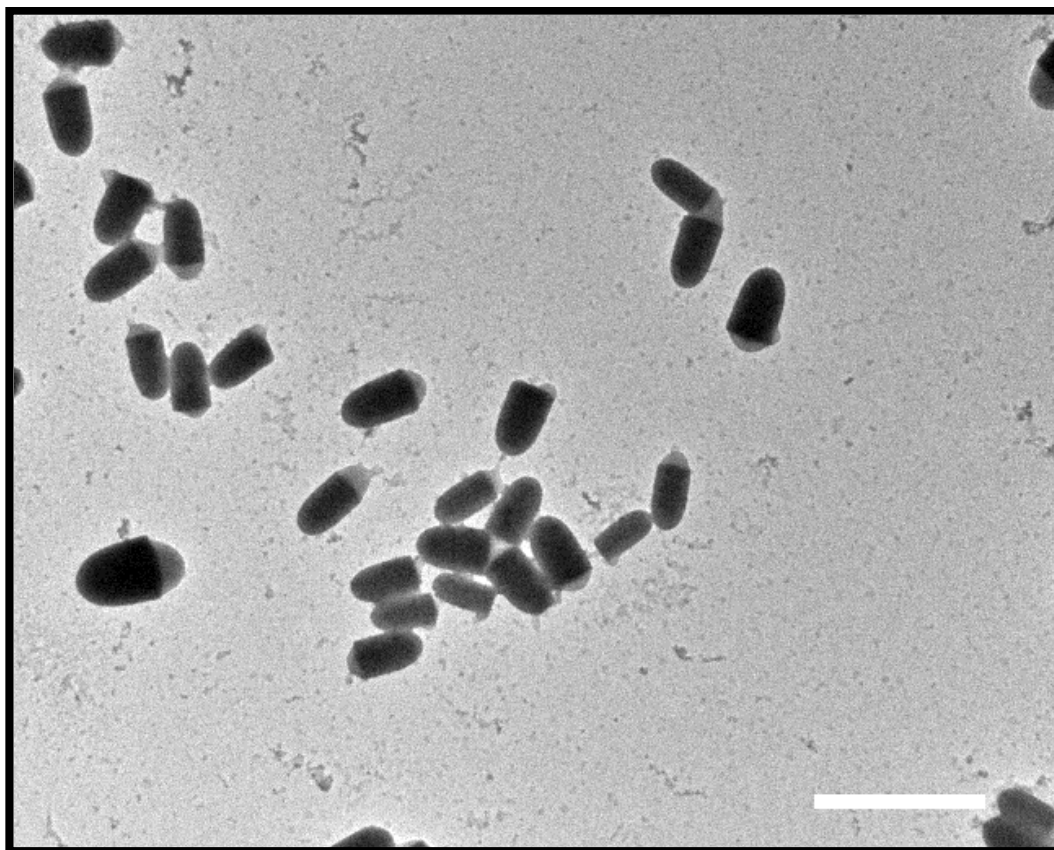


Figure S3. TEM image of hybrid particles obtained 40 minutes after the start of the polymerization of MMA in the presence of silica rods as seeds. Most of the PMMA bulbs are located at the flat surface of the rods. The scale bar is 2 μm .

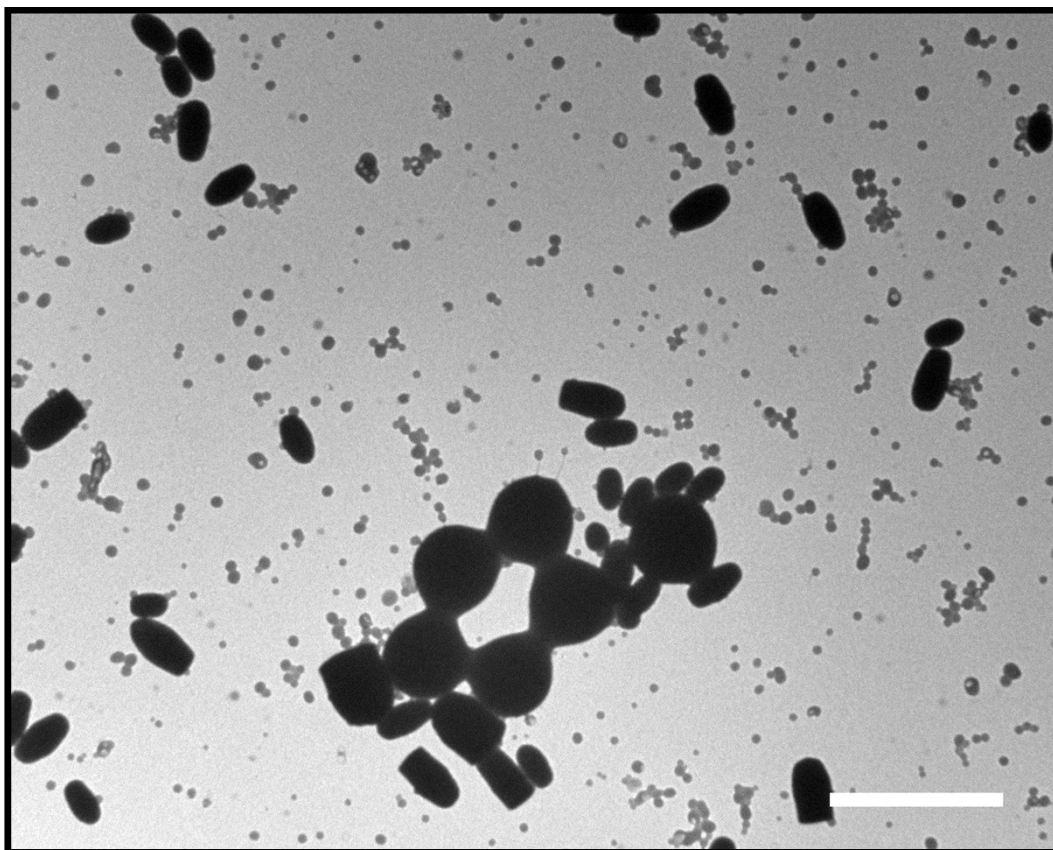


Figure S4. TEM image of a system prepared with bare silica rods (without TPM treatment) and monomer (MMA). Clearly, PMMA did not attach to the rods. The scale bar is 2 μm .

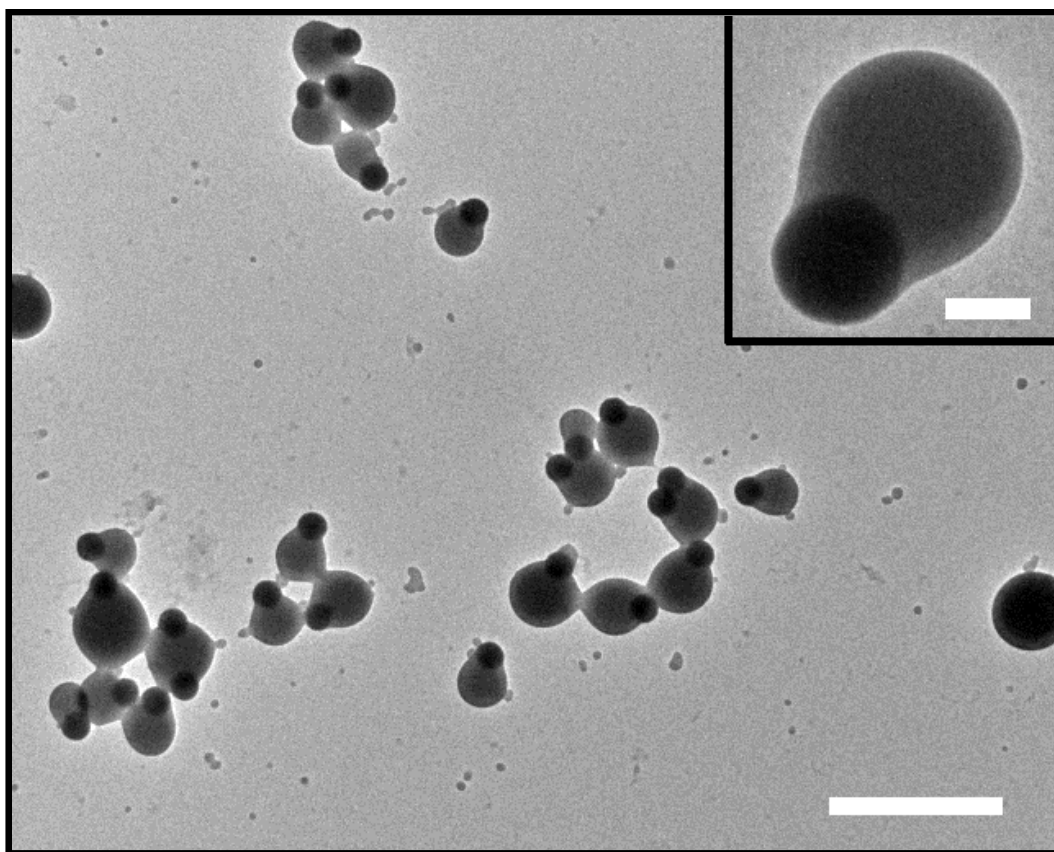


Figure S5. Transmission electron microscopy (TEM) image of snowman-shaped silica-PMMA particles, made by using TPM-SiO₂ spheres instead of the silica rods. It indicates that the TPM modified silica surface was partially wetted with PMMA. The scale bar is 2 μ m in the main figure and 200 nm in the inset, respectively.

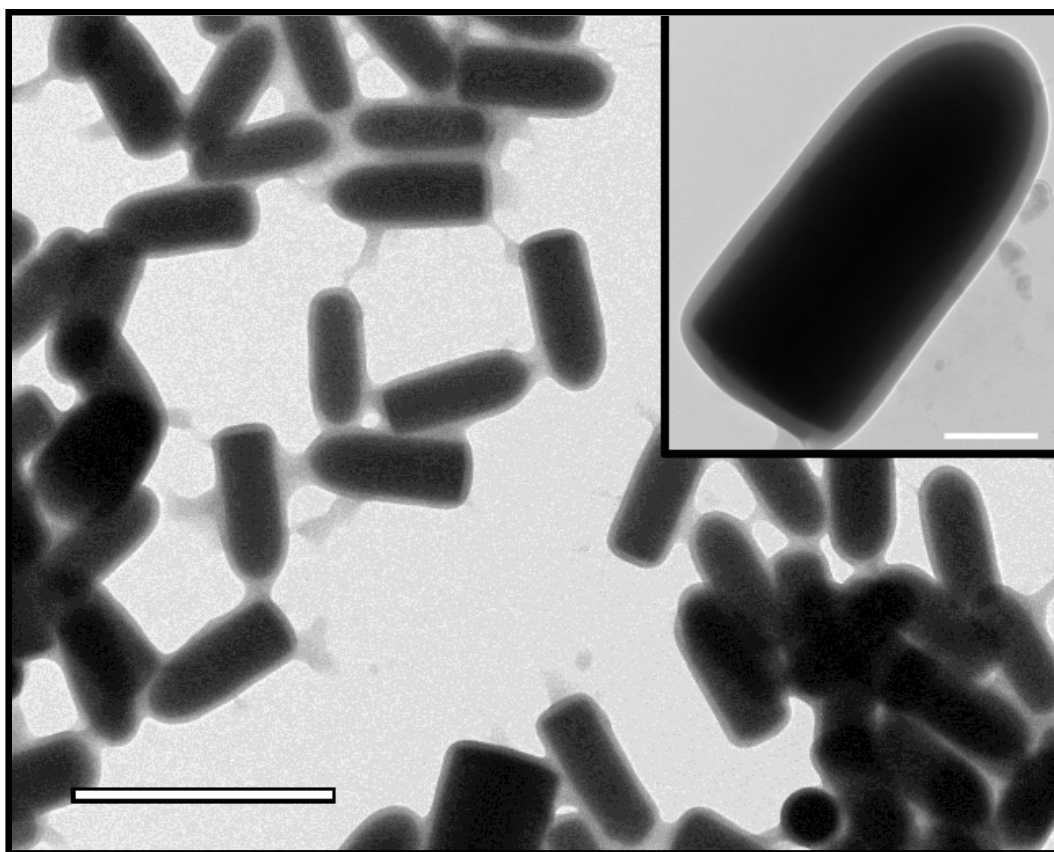


Figure S6. TEM image of core-shell PMMA-silica particles prepared in apolar solvent (mixture of hexane and dodecane, the recipe is originally from supplementary ref. 1). The scale bar is 2 μm in the main figure and 200 nm in the inset, respectively.

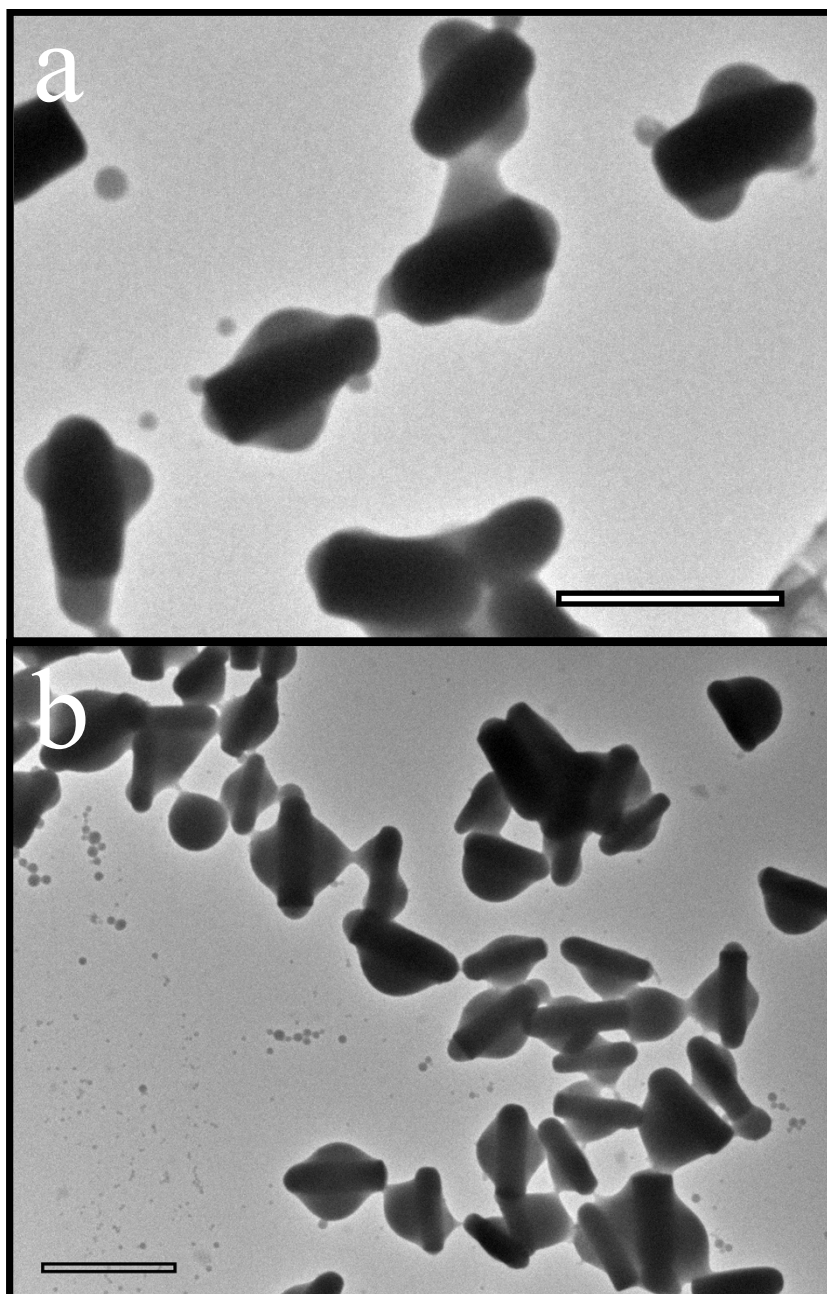


Figure S7. TEM images of PMMA attached silica rods that have been coated with an additional layer of 15 nm of silica. **a**, short rods (aspect ratio is about 2.4). **b**, long rods (aspect ratio is about 3.8). The silica/MMA mass ratio was 9.7:1. The scale bars in a) and b) are 1 and 2 μm , respectively.

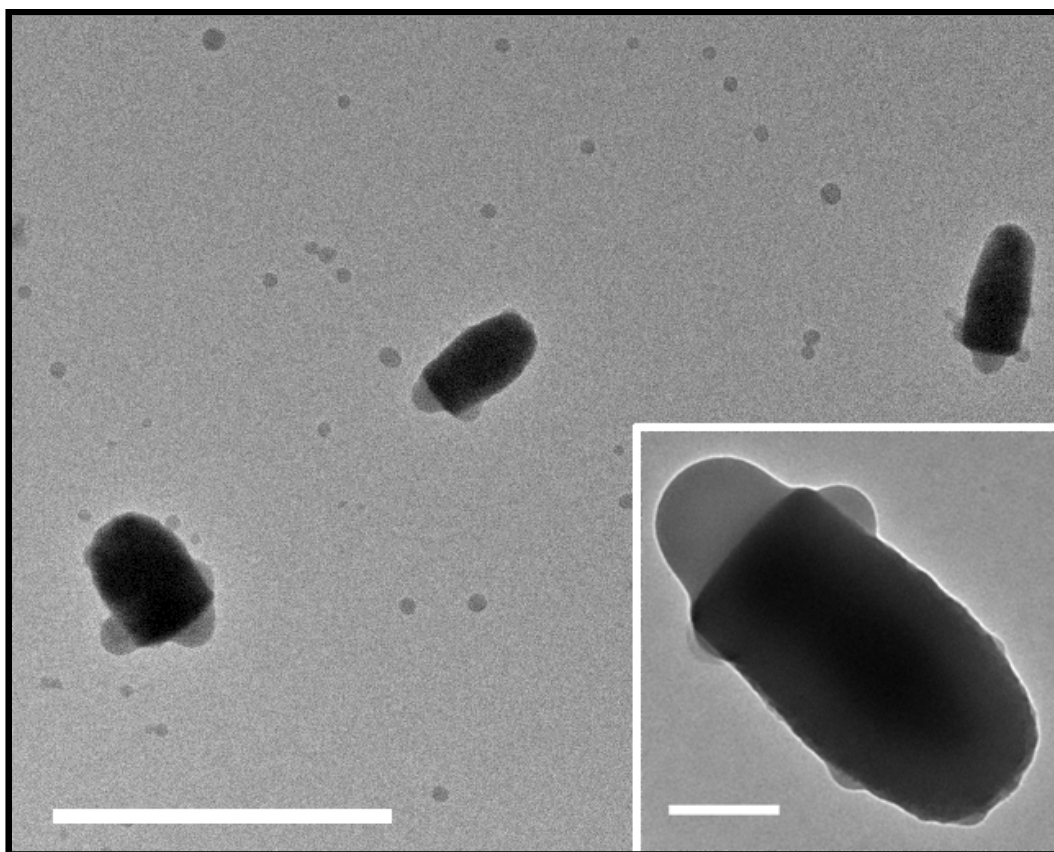


Figure S8. TEM image of lollipop-shaped hybrid particles by using piranha-cleaned silica rods. Most of the PMMA is at the flat end of the silica rods, but small secondary PMMA bulbs are also present. The scale bar is 2 μm in the main figure and 200 nm in the inset, respectively.

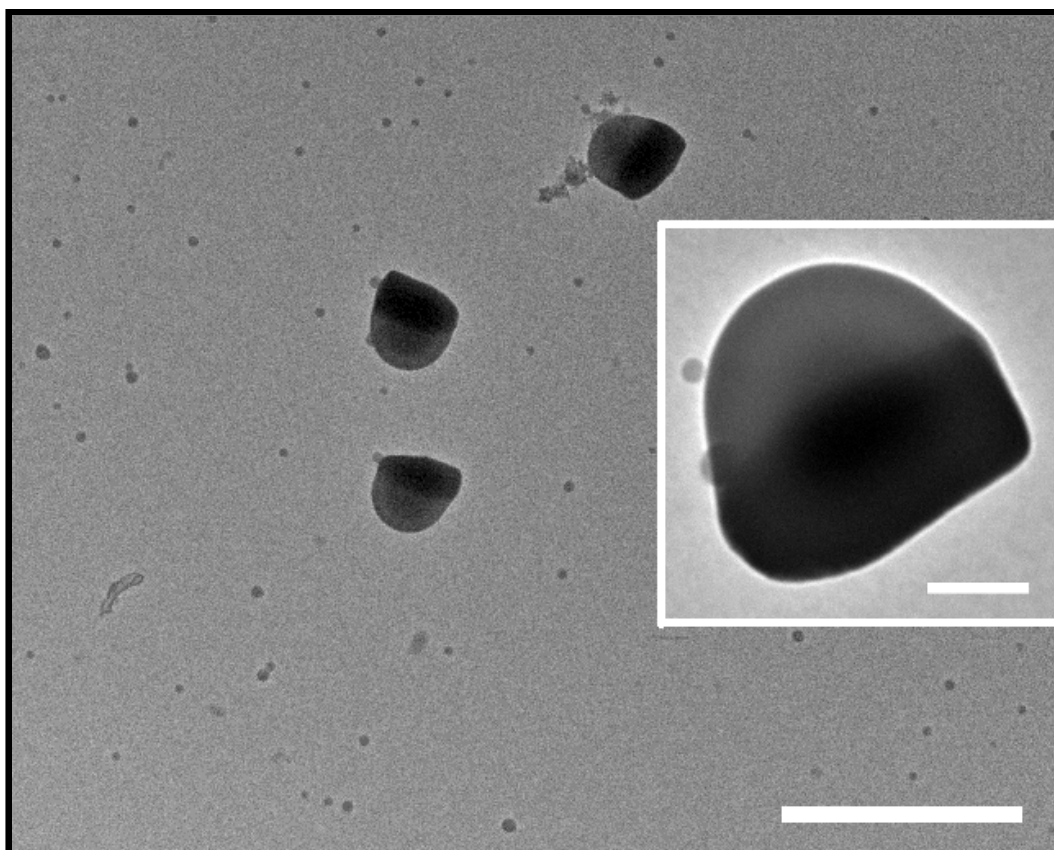


Figure S9. TEM images of PMMA bulbs attached to the silica rods side-on, after the silica rods had been calcined at 500 °C for 2 h. The silica/MMA mass ratio was 9.7:1. The scale bar is 2 μm in the main figure and 200 nm in the inset.

Vectorial orientation of lollipop particles

The lollipop particles showed a clear orientation in the field with their silica rods towards one of the electrodes and their PMMA spheres towards the other. In a field of frequency 400 mHz and strength 15-20 V/mm, the particles followed the field by preferentially rotating the silica rods. In this way, the particles could be aligned ‘vectorially’. The particles turned their silica rods towards one electrode, underwent electrophoresis towards that electrode, and turned around towards the other electrode as the field inverted. A DC field also oriented the particles to one electrode, but such a field quickly induced drift in the samples.

At higher frequencies, on the order of 10 Hz, the particles were unable to follow the field orientation and displayed only Brownian motion. At very high frequencies, on the order of a 1 MHz, the particles were aligned in the field as a result of dipolar interaction with the field, yet the orientation of lollipop-shaped particles was in random.

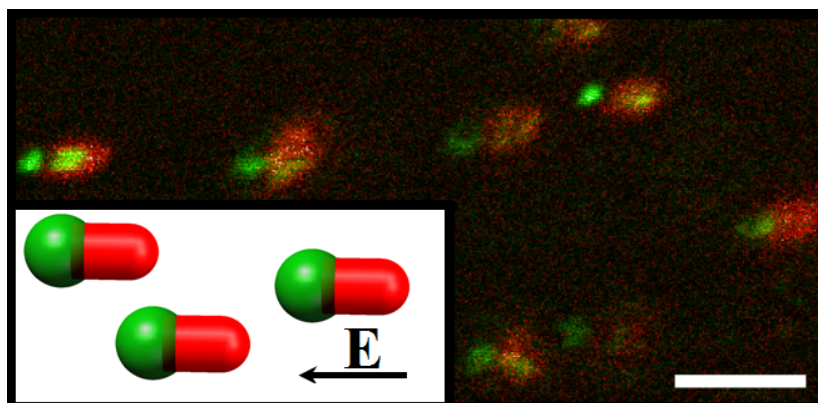


Figure S10. Uniform orientation of anisotropic silica-PMMA particles aligned by electric field (green reflection signal, red fluorescence). The scale bar is 5 μm .

Numerical evaluation of rod-liquid adsorption surface free energies

Rods with homogeneous surface properties

The strategy that we used to determine the behavior of bullet-shaped particles with homogeneous surface properties adsorbed to the flat interface between two liquids is the theoretical method of refs. 43 and 44. This method is the so-called triangular-tessellation technique, in which the surface of the particle is approximated by a large number of small triangles. The quality of the approximation of the object by a triangular mesh can be improved upon by increasing the number of triangles, thereby reducing the size of the individual triangles. In this model, only one particle is considered at a flat fluid-fluid interface. The free energy of adsorption associated with this system is governed solely by the surface areas of fluid-fluid and particle-fluid interfaces, thereby ignoring line tension contributions from the three-phase contact-line. This is in the spirit of the early studies on colloid adsorption by, *e.g.*, P. Pieranski.^{s4} The free energy of adsorption may be written as

$$V(z, \phi) = \gamma_{12}(A - S_{12}) + \gamma_{1c}S_1 + \gamma_{2c}S_2 + \text{const}, \quad (\text{S2})$$

where S_1 is the surface area of the particle with fluid 1 above the interface, while S_2 is the surface area of the particle with fluid 2 below the interface; A is the total surface area between fluid 1 and fluid 2, and S_{12} is the area excluded from that interface by the presence of the particle. γ_{12} , γ_{1c} and γ_{2c} are the surface tensions between phase 1 and 2, and the particle; and the constant in Equation S2 can be tuned to set the energy of the particle completely immersed in fluid 1 to zero. The adsorption free energy in Equation S2 depends through the surface areas on z (the distance of the interface with respect to the center of the particle) and ϕ (the polar angle, which measures the angle between the particle's rotational symmetry axis and the interface normal, ranging from 0 to π). A schematic model can be found in Figure S11.

We define the state in which the particle is fully immersed in phase 1 as a reference state. In this case, the relative free energy is written as

$$F(z, \phi) = V(z, \phi) - \gamma_{12}A - \gamma_{1c}S = (\gamma_{1c} - \gamma_{2c})(S_1 - S) - \gamma_{12}S_{12}, \quad (\text{S3})$$

where S is the total surface area of the particle ($S = S_l + S_2$). When the particle is completely encompassed by phase 1, $F(z, \phi)$ is zero. The $\gamma_{1c} - \gamma_{2c}$ dependence can be written using Young's equation,^{s5}

$$\gamma_{12} \cos \theta = \gamma_{1c} - \gamma_{2c}, \quad (\text{S4})$$

such that Equation S3 becomes

$$F(z, \phi) = \gamma_{12} [(S_1 - S) \cos \theta - S_{12}] \quad (\text{S5})$$

Figure S11. Side view **a** and top view **b** of a bullet-shaped particle adsorbed at a flat liquid-liquid interface, showing the parameters used in our model. The center of particle (point O) is located at a distance z to the interface of phase 1 and phase 2. The polar angle ϕ is the angle between the interfacial normal and the rotational symmetry axis of the particle. The interface has a total area A with corresponding interfacial tension γ_{12} . The surface area of the particle consists of two parts, one is above the interface, of which the size is denoted by S_l with a corresponding surface tension of γ_{lc} between particle and phase 1, the other is below, with contact area S_2 and a surface tension of γ_{2c} between particle and phase 2. The area enclosed by the dashed line in **b** is the cross section S_{l2} of the particle at the interface. The dashed ellipse in **b** is the contact line with a circumference of L , a parameter which will not be used in this study.

Additional details on the numerical calculation of the free energy of adsorption by means of the triangular-tessellation technique are provided in refs. 43 and 44.

According to Equation S5, for a given particle shape, only the interfacial tension (γ_{12}) between phase 1 (methanol) and 2 (PMMA), and the contact angle (θ) are necessary for the free-energy calculation. In order to use this model, certain assumptions have been made: i) the PMMA is regarded as a liquid-like phase at the reaction temperature (55°C), and the

interfacial tension γ_{12} is the surface tension between PMMA and methanol; ii) Due to fact that methanol completely wets solid PMMA,^{s6, s7} the exact value of the interfacial tension is unknown and therefore we examine values in the range 0.1 to 0.0001 N/m;^{s6, s8} iii) the contact angle (θ) between TPM-SiO₂, PMMA and methanol is not significantly changed by the solidification of PMMA, and the presence of PVP in the system, and can thus be determined from the experiment, see below; iv) The line tension contribution is neglected throughout, since it typically has a small value on the order of 10^{-11} N.^{s9, s10}

The contact angle of $115^\circ (\pm 10^\circ)$ is obtained based on the TEM images of samples shown in Figure 1b and c, which was considered to be the valid contact angle (θ_0) on the spherocylindrical surface (shaft of the bullet) after the polymerization stopped. That is, the contact angle present in the nascent stage of the polymer attachment is varying and we deem it inaccurate to use images from this time to evaluate the contact angle, in light of the fact that the polymer is very soft during growth. This variation of the contact angle can be appreciated from Fig. 2. Therefore, the contact angle was measured only after when the polymer bulb stopped growing; it has totally solidified and spilled over sharp edge separating the flat end from the shaft of the bullet. This final value can therefore be considered to be a measure for the contact value (θ_0) on the shaft of the spherocylinder. Furthermore, we assumed that curvature effects would not significantly influence the contact angle measurement.

The adsorption energy minimized with respect to z is plotted as a function of the orientational angle ϕ of the particle in Figure S12. It is seen that a horizontal orientation has a lower free energy than a perpendicular one, and that the two states are separated by a large free-energy barrier. Even if a very small value of interfacial tension γ_{12} is adopted, *e.g.*, 0.0001 N/m,^{s8} the free-energy barrier between the metastable state and the equilibrium state is still significant (715 kT). We also plot the adsorption free-energy barrier as a function of interfacial tension in Figure S13. It clearly shows that the energy barrier depends linearly

upon the interfacial tension, as is also evident from Equation S5. Our result implies that once a rod is attached end-on to a PMMA droplet/bulb, it is unlikely to reorient to a parallel configuration due to thermal fluctuations, despite it not being a thermodynamically favored state. However, since in the hedgehog-like assemblies the bullets are exclusively found in the end-on configuration, the possible stability of the end-on configuration is to be investigated. As also explained in the main text, a possible source of such stability could be a chemical heterogeneity on the surface of the bullet, in particular between the flat bottom and the shaft of these colloids, in light of the preferential nucleation of PMMA on the former.

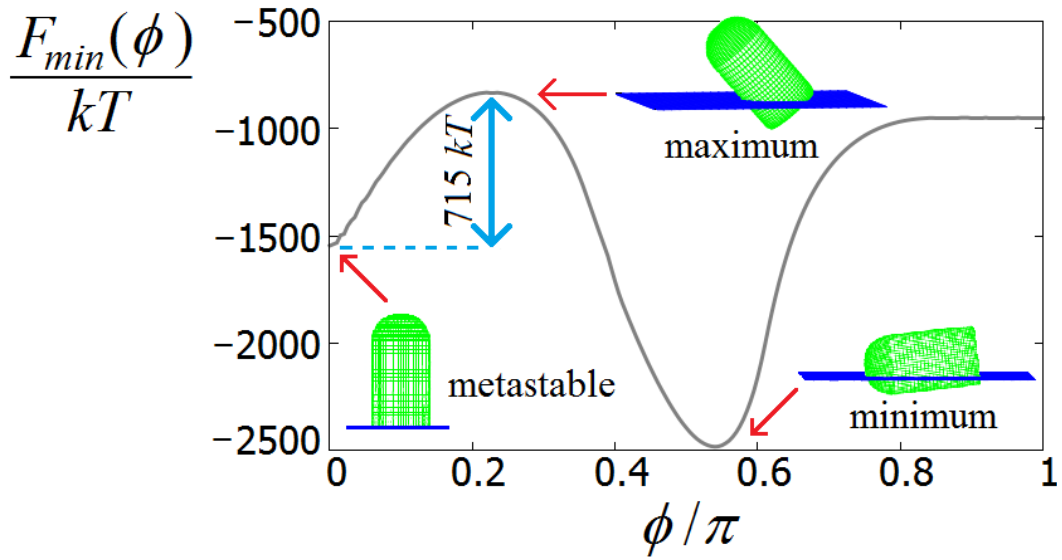


Figure S12. The minimum adsorption free-energy curve (F_{min}) with $\theta = 115^\circ$ and supposed interfacial tension of 0.0001 N/m for the bullet-shaped particle ($L = 737$ nm and $D = 384$ nm) adsorbed at the interface of two liquids. The polar angle between the interfacial normal and the rotational symmetry axis of the colloids is denoted by ϕ (also see Figure S9). The insets show schematic images of the configuration of the particle at the interface, $1kT = 4.11 \times 10^{-21}$ N·m.

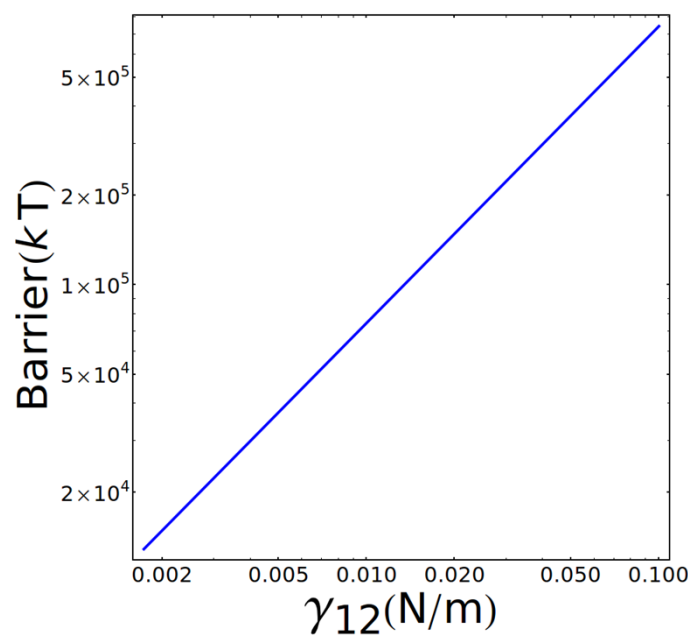


Figure S13. The surface free-energy barrier between the maximum and the metastable minimum as a function of interfacial tension γ_{12} , based on our calculation. The contact angle is 115° .

Rods with heterogeneous surface properties

Our calculation of the free energy of the particles with homogeneous surface chemistry at the flat interface can also be extended to patchy colloid particles, *i.e.*, particles with patches with different surface tensions (see Figure S14).

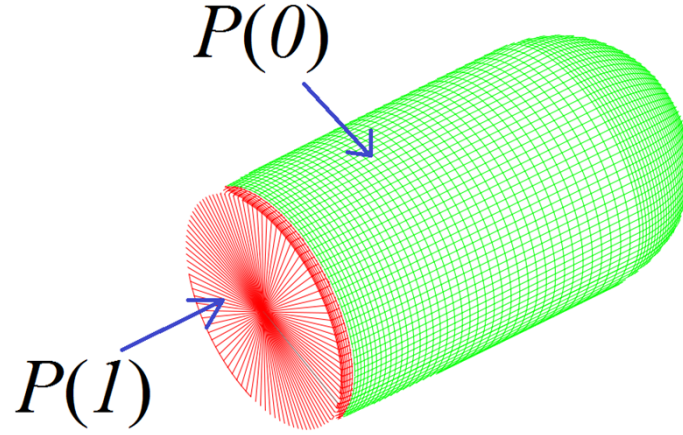


Figure S14. Schematic graph of a patchy colloidal particle.

This means that to every i -th patch we can associate a cosine of the contact angle $\cos\theta_i$. In the case of a colloidal particle with a general shape and with N different patches, its free energy at the interface becomes:

$$F(z, \phi) = \sum_{i=1}^N \gamma_{12} \left[(S_1^{(i)} - S^{(i)}) \cos \theta_i \right] + S_{12} \gamma_{12} , \quad (\text{S6})$$

where $S_1^{(i)}$ is the surface of the i -th patch that is immersed in phase 1, and $S^{(i)}$ is the total surface of the i -th patch.

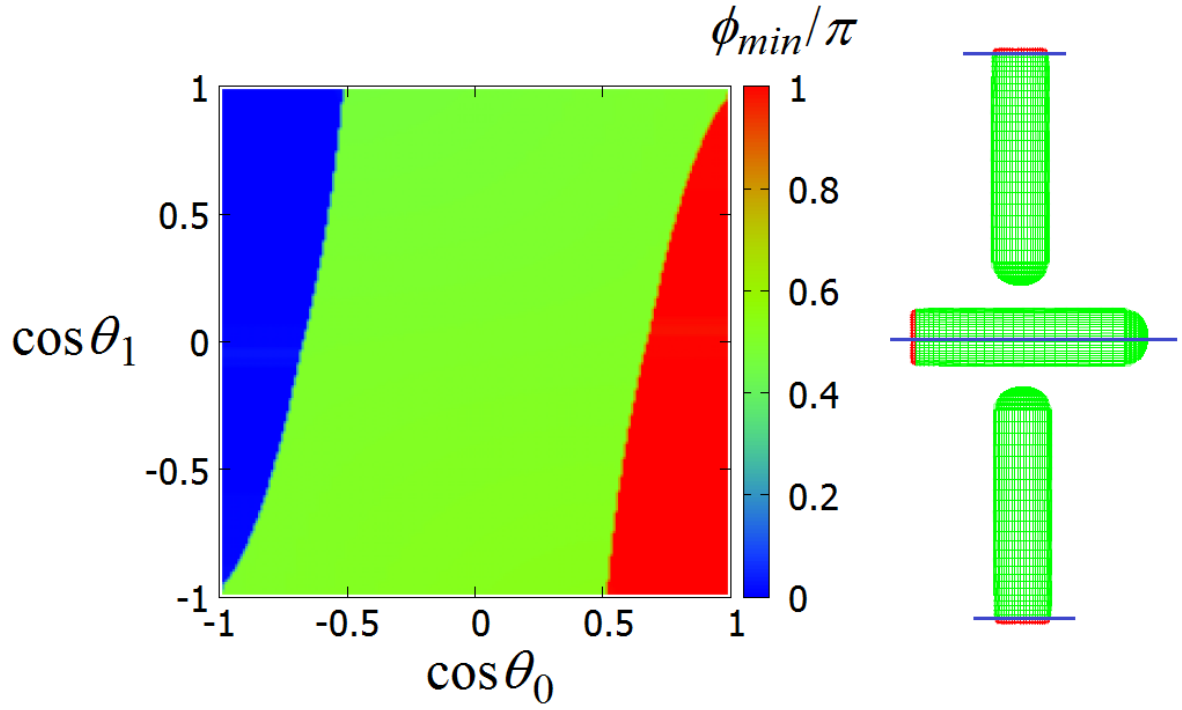


Figure S15. Contour plot of the orientation ϕ (see Figure S9a) of the long rods (aspect ratio is 4.2) configuration with minimum free energy, as a function of the contact angle θ_l (flat base of the bullet-shaped rods) and θ_o (remaining surface).

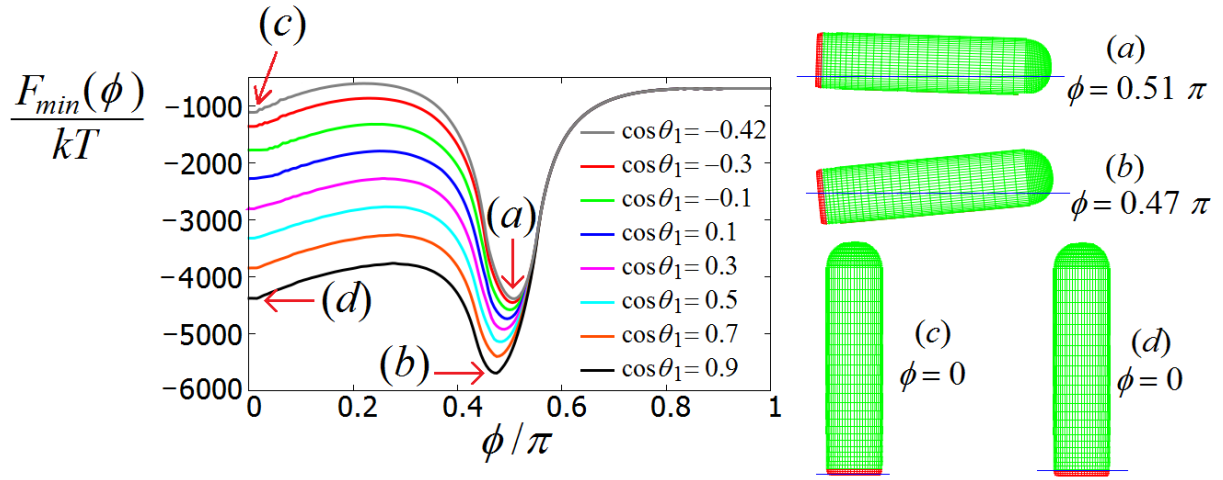


Figure S16. Behavior of a bullet-shaped particle (aspect ratio is 4.2, diameter = 1386 nm and length = 331 nm) adsorbed at the interface with $\cos\theta_0 = -0.42$ and various values of $\cos\theta_1$.

$$1kT = 4.11 \times 10^{-21} \text{ N}\cdot\text{m}.$$

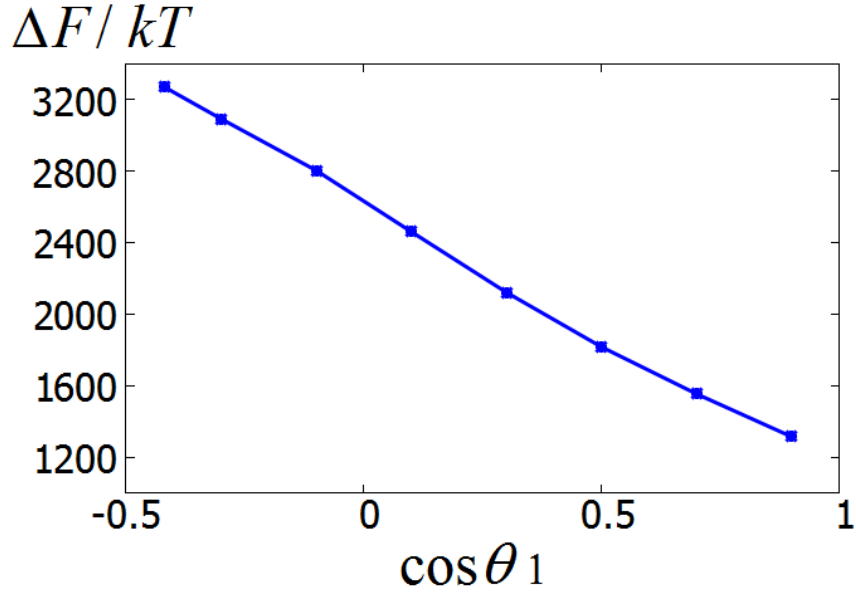


Figure S17. Normalized adsorption free energy difference (Δf) between the metastable and stable state of the bullet-shaped rods (aspect ratio is 4.2) adsorbed at interface.

The relation between the orientation ϕ of the rods with an aspect ratio of 4.2 and contact angles of θ_0 and θ_1 is plotted in Figure S15. Similar to the short rods (aspect ratio is 1.9), there are two distinct regions present where the end-on attachment of the rod to the interface is preferred. However, when $\cos \theta_0$ assumes the value of -0.42 from the experimental observation, the only stable configuration of rods with minimum adsorption free energy is always the side-on attachment to the interface regardless of the value of θ_1 (see Figure S16). This is clearly shown in Figure S17, where the normalized adsorption free energy difference (ΔF) remains positive. Thus, we can conclude that the surface chemistry heterogeneity on a long bullet is not sufficient to stabilize the end-on attachment on the interface.

Supplementary references

- [1] L. Antl, J. W. Goodwin, R. D. Hill, R. H. Ottewill, *Colloids and Surface* **1986**, *17*, 67.
- [2] A. P. Philips, A. Vrij, *J. Colloid Interface Sci.* **1989**, *128*, 121.
- [3] U. Dassanayake, S. Fraden, A. van Blaaderen, *J. Chem. Phys.* **2000**, *112*, 3851.
- [4] P. Pieranski, *Phys. Rev. Lett.* **1980**, *45*, 569.
- [5] T. Young, *Phil. Trans. R. Soc. Lond.* **1805**, *95*, 65.
- [6] J. R. Dann, *J. Colloid Interface Sci.* **1970**, *32*, 302.
- [7] A. Zdziennicka, *Colloid Surface A.* **2010**, *367*, 108.
- [8] W. A. Zisman, in *Contact Angle, Wettability, and Adhesion*, Vol. 43 (Ed: F. M. Fowker), American Chemical Society, Washington, DC, **1964**, pp. 1-51.
- [9] J. S. Rowlinson, B. Widom, *Handbook of Surface and Colloid Chemistry*; Dover Publication, Midneola, 1st edition, **2003**.
- [10] A. Amirfazli, A. W. Neumann, *Adv. Colloid Interface Sci.* **2004**, *110*, 121.